Amplitude and Frequency Characteristics of a Ring Laser

T. J. HUTCHINGS, J. WINOCUR, R. H. DURRETT, E. D. JACOBS, AND W. L. ZINGERY
Autonetics, a Division of North American Aviation, Incorporated, Anaheim, California
(Received 3 June 1966)

The variations in intensity and difference frequency of the oppositely directed traveling waves in a ring laser with a single isotope and with mixed isotopes of neon have been measured as a function of cavity tuning. Agreement with the theory of F. Aronowitz and C. V. Heer is obtained. Amplitude modulations of each beam intensity at the difference frequency are observed. The sum intensity shows a power dip and no modulation. Complete extinction of one traveling wave over narrow frequency bands separated by one half of the mode spacing is observed. In two-mode operation the observed extinction width is less than 1 Mc/sec.

I. INTRODUCTION

THE variations in intensity and difference frequency of the oppositely directed traveling waves in a ring laser with a single isotope and with mixed isotopes of neon have been measured as a function of cavity tuning. The results are compared with the theory of Aronowitz[1] and Heer.[2] Qualitative agreement, which probably could be improved by inclusion of collision effects[3] in the theory, was obtained. An amplitude modulation of each beam intensity at the applied bias frequency was observed. This effect permits the observation of the difference frequency with signal-to-noise characteristics that are comparable to those of the observed heterodyne beat signal. In addition, some interesting mode-extinguishing effects were observed that are useful for stabilization of the laser frequency.

The observed effects of mode pushing and pulling on the amplitudes and difference frequencies are particularly useful for evaluating the ring laser as a precision instrument for measurement of rotation rate in inertial space,[4] and are relevant to the study of laser statistics,[5] and oscillator linewidth.[6]

II. COMPUTATIONS OF MODE AMPLITUDES AND FREQUENCIES

In a formal treatment of the traveling-wave ring laser, Aronowitz derives a set of equations that determine the amplitudes and frequencies of oscillation of the counter-rotating traveling waves of a ring laser operating in a single longitudinal mode. His method is a modification of Lamb's standing-wave formulation[7] that allows the treatment of both the traveling- and the standing-wave laser. The steady-state solutions to the self-consistent amplitude-determining equations may be solved for the dimensionless intensities

$$I_i=|\mu_{ab}|^2E_i^2/(2\hbar^2\gamma_a\gamma_b),\quad i=1,2 \tag{1}$$

of the counter-rotating waves, where μ_{ab} is the matrix element of the electric dipole moment taken between states a and b, γ_a and γ_b are the spontaneous decay rates from these states, and E_i is the electric field strength. The result for a mixture of two isotopes of masses m and m' is (for $d\gg\gamma_{ab}$)

$$\begin{aligned}I_i=\{&[Fe^{-x_i^2}+F'e^{-x_i'^2}-N_i^{-1}][Fe^{-x_j^2}+F'e^{-x_j'^2}]\\&-[Fe^{-x_j^2}+F'e^{-x_j'^2}-N_j^{-1}]\\&\times[Fe^{-x_i^2}L(x)+F'e^{-x_i'^2}L(x')]\}\\&\times\{F^2e^{-(x_i^2+x_j^2)}[1-L^2(x)]\\&+F'^2e^{-(x_i'^2+x_j'^2)}[1-L^2(x')]+FF'[1-L(x)L(x')]\\&\times[e^{-(x_i^2+x_j'^2)}+e^{-(x_i'^2+x_j^2)}]\}^{-1},\\&(i=1,\ j=2;\ i=2,\ j=1).\end{aligned} \tag{2}$$

Here $x_i=(\nu_i-f_d)/d$, $i=1, 2$, where ν_i is the oscillation frequency of one of the counter-rotating traveling waves, f_d is the atomic transition frequency, d is the Doppler width divided by $2(\ln 2)^{1/2}$, N_i is the ratio of population inversion to threshold inversion, F is the fraction of the total number of atoms with mass m,

$$L(x)=[1+(xd/\gamma_{ab})^2]^{-1}, \tag{3}$$

$$x=\tfrac{1}{2}(x_1+x_2), \tag{4}$$

$$\gamma_{ab}=\tfrac{1}{2}(\gamma_a+\gamma_b), \tag{5}$$

and

$$F'=(m'/m)^{1/2}(1-F). \tag{6}$$

The steady-state solution of the frequency determining equations for two isotopes (for $d\gg\gamma_{ab}$) is

$$\nu_i=f_i+N_1[FJ(x_i,x_j)+F'J(x_i',x_j')],\quad(i=1,\ j=2;\ i=2,\ j=1), \tag{7}$$

where

$$J(x_i,x_j)=(\Delta\nu_c/2)\left[-\frac{2}{\sqrt{\pi}}\left(\int_0^{x_i}e^{s^2}ds\right)e^{-x_i^2}+\frac{xd}{\gamma_{ab}}I_je^{-x_j^2}L(x)\right], \tag{8}$$

[1] F. Aronowitz, Phys. Rev. **139**, A635 (1965).
[2] C. V. Heer, Colloque sur le Progrès des Gyroscopes, Centre National d'Etudes Spatiales, 1964 (unpublished).
[3] B. L. Gyorffy and W. E. Lamb, Jr., *Physics of Quantum Electronics*, edited by P. Kelley, B. Lax, and P. Tannenwald (McGraw-Hill Book Company, Inc., New York, 1966), p. 602.
[4] W. Macek and D. Davis, Appl. Phys. Letters **2**, 67 (1963).
[5] V. Letokhov and E. Markin, Zh. Eksperim. i Teor. Fiz. **48**, 770 (1965) [English transl.: Soviet Phys.—JETP **21**, (1965)].
[6] J. Winocur, M. C. Suman, R. H. Durrett, E. D. Jacobs, T. J. Hutchings, and W. L. Zingery, Bull. Am. Phys. Soc. **10**, 129 (1965).
[7] W. E. Lamb, Jr., Phys. Rev. **134**, A1429 (1964).

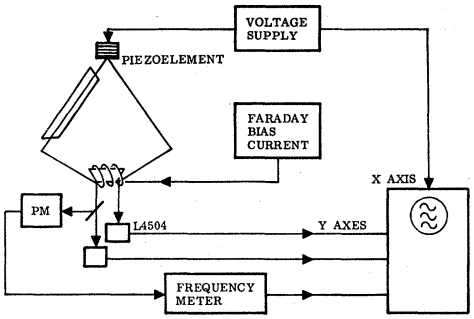

FIG. 1. Block diagram of measuring apparatus.

and f_i ($i=1, 2$) is the cavity frequency of the traveling wave having intensity I_i. The Ne^{20}-Ne^{22} isotope shift $f_d-f_{d'}$ has been measured to be 875 Mc/sec for the 6328 Å transition, with Ne^{22} on the high-frequency side.[8]

Computer solutions were obtained here of both the amplitude equations (2) and the frequency equations (7) for unequal as well as for equal gain to loss ratios of the counter-rotating traveling waves. These solutions show for a ring laser with a single isotope that extinction of one traveling wave may occur over a narrow range of frequencies

$$\Delta f=\frac{8\gamma_{ab}^2}{d^2}\frac{N}{N-1}|f_2-f_1|, \qquad (9)$$

when the gain-to-loss ratios for radiation traveling in either direction are equal ($N_1=N_2=N$). When the gain-to-loss ratios are slightly unequal then the range of unidirectional oscillation is given by

$$\Delta f\cong 2\gamma_{ab}\left[\frac{N_1-N_2}{N_1(N_2-1)}\right]^{1/2}, \quad (N_1>N_2) \qquad (10)$$

and may be many Mc/sec.

The effects of mode pushing and pulling expressed by Eq. (7) cause the counter-rotating traveling waves to deviate unequally from their respective cavity frequencies, resulting in a difference frequency error that is a function of cavity tuning. This error is conveniently written in terms of a coefficient $a(f_1,f_2)$ defined here as

$$a(f_1,f_2)=\frac{(\nu_2-\nu_1)-(f_2-f_1)}{f_2-f_1}. \qquad (11)$$

III. APPARATUS

The ring laser used in these experiments employs three prism reflectors, each having a back surface radius of curvature of 90 cm. The laser tube has an active length of 11 cm with a bore diam of 0.15 cm and is filled with a 90–10 mixture of He^3-Ne^{20} to a total pressure of 2.5 mm Hg. The isotopic purity of the Ne^{20} is greater than 99.5%. An alternate tube with an equal mixture of Ne^{20}-Ne^{22} in place of the Ne^{20} was also used. A short section at each end of the thick-wall-quartz laser tube is counterbored to permit more efficient coupling of the 40.68 Mc/sec rf energy.[9] The windows are optically contacted at Brewster's angle.

The laser cavity is constructed of brazed tubular Invar. Cavity-length adjustments are made via a heater element mounted on one arm of the cavity and by control of a piezoelectric transducer supporting one of the prism reflectors. A specially designed Faraday element performs three simultaneous functions: (1) It generates a bias frequency by introducing a nonreciprocal phase difference between the counter-rotating waves; (2) it selects the frequency of operation, in this case 6328 Å, by refracting the 1.15 μ and the 3.39 μ lines from a closed path; and (3) it provides an optical pickoff via 0.05% reflection from the nearly Brewster-angle front surfaces. By proper matching of refractive indices, there are negligible back reflections from the quarter-wave plate-to-glass interfaces of the Faraday element.

A small circular aperture reduces the effective Fresnel number of the cavity with minimum back scatter, and permits operation in the TEM_{00} mode. The intermode beat frequency is 510.6 Mc/sec. Single longitudinal-mode operation is obtained by appropriate gain reduction. The ring-laser rotation scale factor was measured using a precision tilt table to be 1.00 cps/(arc sec/sec), in agreement with the value calculated for a ring laser containing different optical media.[10]

The system used to measure mode intensities and beat frequencies is shown in Fig. 1. The bias frequency is detected as an amplitude modulation on one of the two counter-rotating waves and is measured by a Hewlett-Packard, Inc. 500B frequency meter whose output is displayed on an oscilloscope. The wave amplitudes are detected by Philco L4504 photodiodes and simultaneously displayed on the oscilloscope. The X axis of the scope is driven by the voltage supply responsible for sweeping the laser cavity via the piezoelectric transducer.

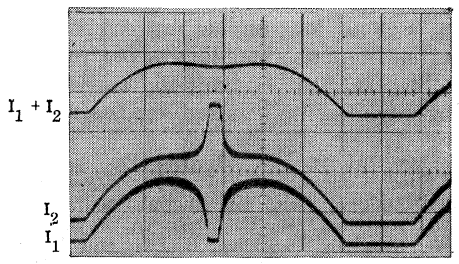

FIG. 2. Experimental display of oppositely directed traveling wave intensities I_1, I_2 and sum intensity I_1+I_2 versus cavity tuning showing amplitude modulation and extinction phenomena in single mode operation. The mode spacing is 510 Mc/sec.

[8] R. Cordover, T. Jaseja, and A. Javan, Appl. Phys. Letters **7**, 322 (1965).

[9] J. A. Collinson, Bell System Tech. J. **44**, 1511 (1965).

[10] C. V. Heer, Phys. Rev. **134**, A799 (1964).

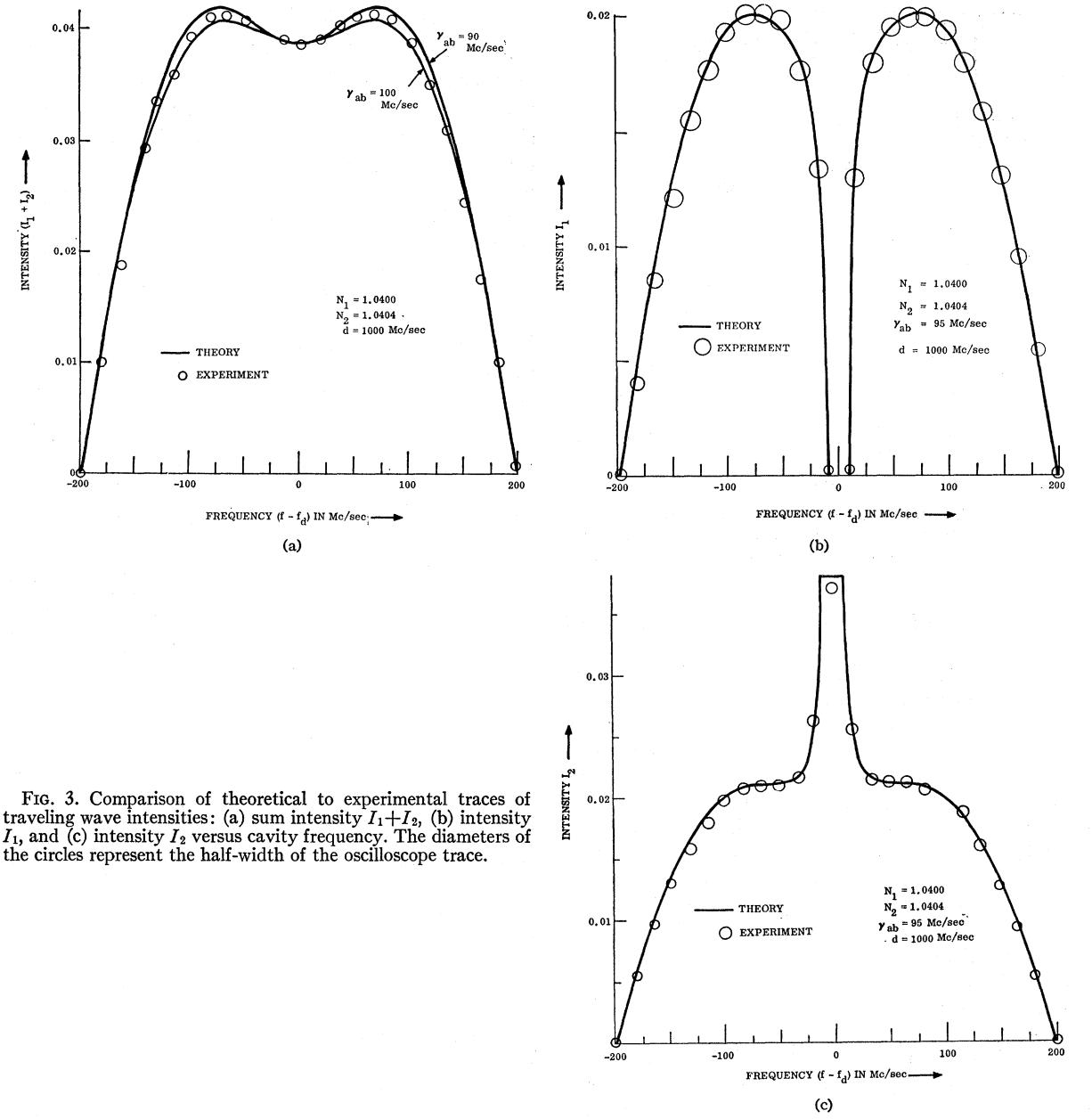

FIG. 3. Comparison of theoretical to experimental traces of traveling wave intensities: (a) sum intensity I_1+I_2, (b) intensity I_1, and (c) intensity I_2 versus cavity frequency. The diameters of the circles represent the half-width of the oscilloscope trace.

IV. EXPERIMENTAL RESULTS

A. Intensity Modulation

When a Faraday bias is applied to the ring laser, a frequency difference between the counter-rotating traveling waves is generated that is proportional to the applied magnetic field intensity. This difference frequency can be observed as a beat frequency by standard heterodyne techniques. In the experimental ring laser this difference frequency was observed as an amplitude modulation on the wave intensities. Each wave is modulated at the difference frequency with a phase relationship of exactly 180°. The sum of the two-wave intensities has no detectable first-harmonic component. The electric field amplitude of each traveling wave may be written as

$$A_i(t)=E_i(t)[\cos\omega_i t+\phi_i(t)], \quad i=1,2, \qquad (12)$$

where $\omega_i=2\pi f_i$. The observed intensity modulation may be described by an electric field amplitude of the form

$$E_i(t)=E_i'+E_i''\sin(\omega_2-\omega_1)t, \quad i=1,2, \qquad (13)$$

with $E_1'=E_2'$ and $E_1''=-E_2''$. Because of the 180-deg phasing of the amplitude modulations, there is negli-

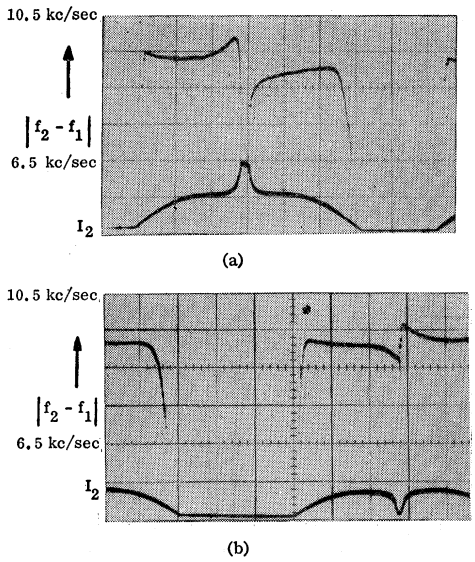

FIG. 4. Experimental displays of difference frequency and wave intensity for (a) the counterclockwise wave dominant and (b) the counterclockwise wave extinguished at the center of the gain curve.

gible distortion of the conventional heterodyne beat signal.

The origin of the amplitude modulation is believed to be an interaction within the laser cavity between one traveling wave and back scattered radiation from the second traveling wave. When light is intentionally back reflected from one wave to the other by an external mirror, the amplitude of the oscillations is found to increase by an order of magnitude with only 2×10^{-8} of the original power reflected back into the cavity. In a standing wave laser there are pulsations in the second-order population inversion density at the intermode frequencies under multimode operation.[7] No analogous effect is predicted in a non-degenerate single mode ring laser in the absence of coupling.[1,2]

Large amplitude oscillations have been observed in a small region (typically <20 Mc/sec) about the center of the gain curve with no applied bias. The two-wave intensities are exactly out of phase just as in the case of an applied bias. The oscillation frequency is always greater than the "locking frequency" of the ring laser, which is about 500 cps. These oscillations are thought to be identical in origin to the "bias beats" observed by Heer as a heterodyne beat signal.[11] They result from the coupling of energy from one traveling wave into the oppositely directed traveling wave due to scattering. The theory predicts that the "bias beat" frequency increases as the cavity is tuned in the direction of the atomic transition frequency.[11] When the "bias beat" frequency exceeds the locking frequency, oscillations may occur.

[11] C. V. Heer, Symposium on Unconventional Inertial Sensors, Polytechnic Institute of Brooklyn Graduate Center, New York, 1964 (unpublished).

B. Single-Isotope Results

A typical experimental display of wave intensity versus cavity tuning for an isotopically pure ring laser, with constant applied Faraday bias, operating in a single longitudinal mode is shown in Fig. 2. The counterclockwise wave (bottom) is completely extinguished in a narrow region at the center of the gain curve. The width of this extinction region decreases with increased power in agreement with Eq. (10). Incomplete extinction may occur when the gain to loss ratios of the oppositely directed traveling waves are more nearly equal. The clockwise wave (middle) exhibits a corresponding intensity increase so that the electronic sum of the two intensity signals (with selective amplification) yields a total output intensity I_1+I_2 (top) that has the well known "power dip" typical of a standing wave laser. Amplitude modulations are evident in the clockwise and counterclockwise waves but are absent in the electronic sum due to cancellation. In Figs. 3(a), 3(b) and 3(c), the experimental curves are magnified and compared to the theoretical plots. The average gain-to-loss ratio $N=\frac{1}{2}(N_1+N_2)$ is determined from the 398 Mc/sec oscillation range and the assumed $d=1000$ Mc/sec emission linewidth to be 1.040. The depth of the power dip is quite sensitive to the lifetime parameter γ_{ab} as shown by Fig. 3(a) in which I_1+I_2 is plotted for slightly differing values of γ_{ab}. The best experimental value of γ_{ab} is 95 Mc/sec. The computer curves of Figs. 3(b) and 3(c) show good agreement with the experimentally measured wave intensities if $N_2-N_1=0.0004$.

Figure 4(a) shows a typical oscilloscope trace of difference frequency (top) and traveling wave intensity (bottom) for constant applied bias and single-mode operation. Figure 4(b) shows that the symmetry of the difference frequency curve reverses if the direction of the dominant traveling wave also reverses. A similar effect occurs if the sense of the Faraday bias is reversed but the direction of the dominant wave is unchanged. The experimental values of the traveling-wave gain-to-loss ratios are easily determined from the intensity curves and the previously measured value of γ_{ab}. Figure 5 compares the computer plot of the fractional difference error, $a(f_1,f_2)$, with the experimental curve of Fig. 4(a) for $N_1=1.0370$, $N_2=1.0373$, and an assumed cavity width of 3 Mc/sec. A probable zero level of the experimental curve was selected. Calculation of the actual zero level requires a precise measurement of the cavity difference frequency, f_2-f_1, which was not attempted. The theoretical curve has a form similar to that of the experimental curve, but its magnitude is several times less. This discrepancy may be due to the neglect in the theoretical formulation of effects of collisions between atoms of the active medium. These collisions affect the power dip in two ways. Hard collisions, during which the phase of the interacting Ne atom is completely interrupted, give rise to a line-broadening effect that is

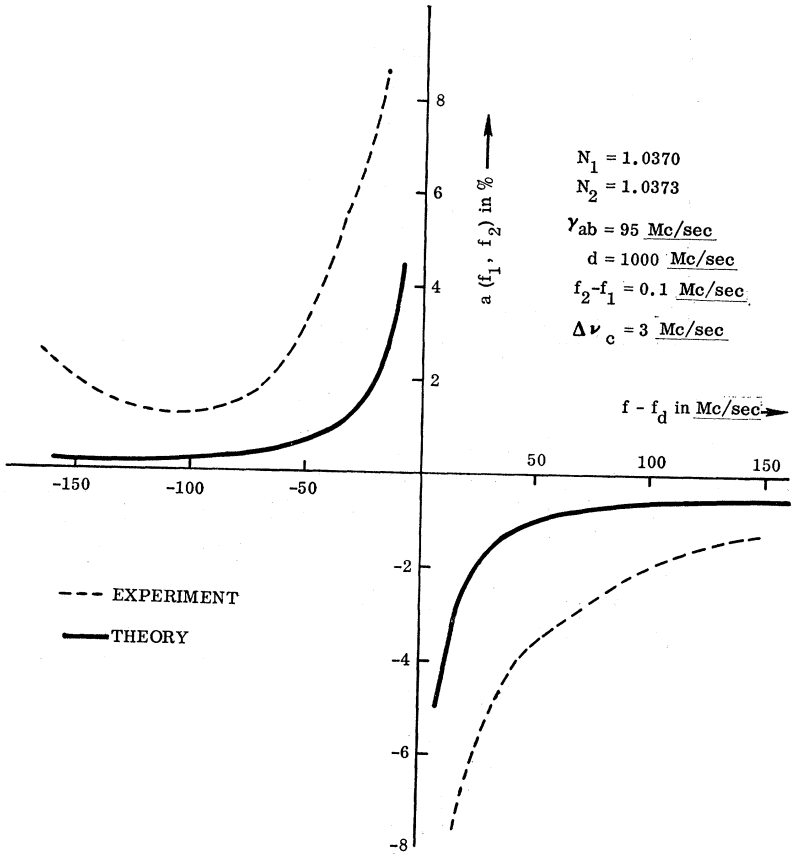

FIG. 5. Comparison of theoretical to experimental traces of error coefficient.

equivalent to an increase in the value of γ_{ab}. Soft distant collisions, for which the wave function of the excited Ne atom remains essentially unaffected, cause a response that resembles an inhomogeneous-type broadening. Although the wave intensities can be described in terms of an effective γ_{ab}, the frequency equations cannot be characterized by the same effective γ_{ab}.

The relative losses of the counter-rotating waves are not controlled in the experiment. They are determined by the unequal scattering from opposite sides of dust particles and optical imperfections in the optical path. During the warmup period the relative wave intensities change rapidly due to changes in the optical path resulting from thermal expansion of the invar frame. With thermal control of the laser cavity length, and with an applied Faraday bias, the relative wave intensities do not change appreciably over many hours. The operation is less stable when no Faraday bias is applied.

When the traveling-wave intensities are almost equal, each wave intensity exhibits a power dip and no wave extinction as shown by the oscilloscope trace in Fig. 6 (bottom), and the difference frequency (top) exhibits little variation with cavity tuning. The computer plot of Fig. 7 illustrates how small the theoretical difference frequency error may be for identical gain-to-loss ratios of the traveling waves.

When the laser excitation is increased to permit two-mode operation, intensity curves of the type shown in Fig. 8 are observed. The depth of the dip in the sum-intensity curve (top) increases with excitation level as expected. This curve agrees very well with the theory for $N = 1.085$ and a value of γ_{ab} roughly 10% larger than the value determined at the lower excitation level. An intensity dip of one traveling wave (bottom) occurs at the center of the gain curve where only one mode is oscillating. Complete extinction occurs at each side of the gain curve where there is a symmetric displacement of two modes. The width of this region over which one traveling wave is extinguished may be less than 1 Mc/sec, while for a single mode at the center of the gain

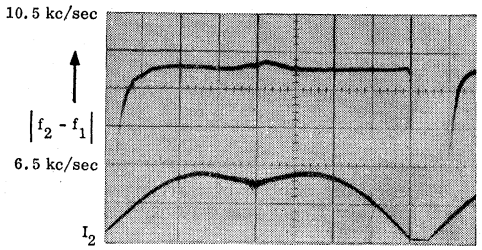

FIG. 6. Experimental display of difference frequency (top) and one wave intensity (bottom) for nearly identical traveling wave intensities.

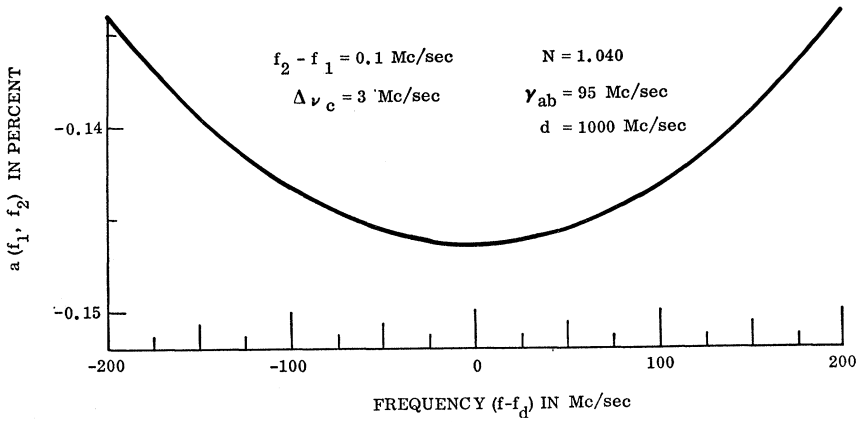

FIG. 7. Theoretical plot of error coefficient $a(f_1,f_2)$ versus cavity frequency for equal gain to loss ratios of the oppositely directed traveling waves.

curve the extinction width is of order 10 Mc/sec. Unlike the effect at the center of the gain curve, the width of the extinction region in the two-mode case decreases with decreasing power level. The extinction region, which appears as a spike in Fig. 8, is shown on an expanded scale in Fig. 9.

Unidirectional oscillations have been observed previously for each λ change in optical path length in a traveling-wave ring laser using all plane mirrors and operating at 3.39 μ.[12] The reason that extinction was not observed at intervals of $\frac{1}{2}\lambda$ as in the present experiment may be the difficulty of observing the very narrow band extinction regions that occur for symmetric two-mode operation.

The origin of mode extinction can be understood pictorally in terms of the "hole burning" theory formulated by Bennett.[13] At the atomic-transition frequency, f_d, the two holes burnt into the gain curve by the counter-rotating waves of a single mode exactly overlap, and the initially stronger wave dominates. For a symmetric placement of two modes, say q and $q+1$, the clockwise wave of the $q+1$ mode competes for atoms with the counterclockwise wave of the q mode, and the clockwise wave of the q mode competes for atoms with the counterclockwise wave of the $q+1$ mode. The initially stronger wave dominates, resulting in unidirectional oscillation in both the q and $q+1$ modes. The origin of the very narrow width of the wave extinction and its observed power dependence lies in the additional competition between the q and $q+1$ modes that occurs for very slight detuning from a symmetric placement of modes.

The application of this phenomenon to the frequency stabilization of a gas laser is obvious. The width of the traveling-wave extinction region is two orders of magnitude narrower than the width of the dip in the sum intensity curve. A corresponding increase in stability should be available over some of the conventional stabilization techniques that utilize the frequency characteristics of the ordinary power dip.[14]

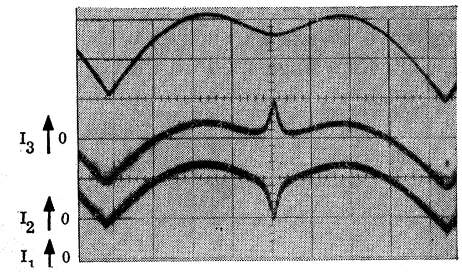

FIG. 8. Experimental displays of traveling-wave intensities I_1, I_2, and sum intensity I_1+I_2 versus cavity tuning showing two-mode extinction effects.

C. Mixed-Isotope Results

The presence of a second Ne isotope can significantly alter the traveling-wave amplitude and frequency solutions. When $N_1=N_2$, the presence of trace amounts of an additional isotope can remove the wave extinguishing instability, and can cause a discontinuity in the error coefficient $a(f_1,f_2)$ near the central frequency of the gain curve as shown by Fig. 10. When $N_1\neq N_2$, small impurities have negligible effects on both the amplitude and the frequency solutions. In this case, a large admixture of a second isotope is required to prevent wave extinction. Figures 11(a) and 11(b) compare the

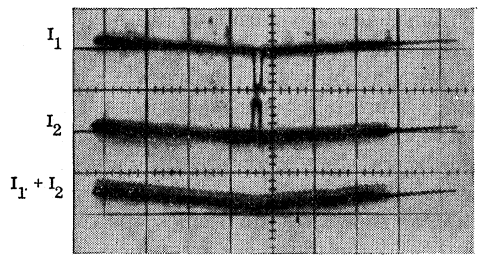

FIG. 9. Enlargement, showing shape and width of two-mode extinguishing region. The frequency scale is 7 Mc/sec per division.

[12] T. Moss, D. Killick, and E. de la Perelle, Infrared Phys. 4, 209 (1964).
[13] W. R. Bennett, Jr., Phys. Rev. 126, 580 (1962).
[14] A. D. White, IEEE J. Quantum Electron. QE-1, 349 (1965).

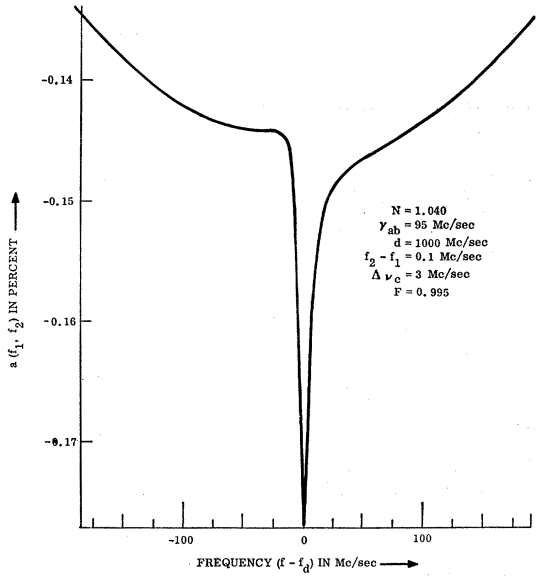

FIG. 10. Theoretical plot of error coefficient $a(f_1,f_2)$ versus cavity frequency for 99.5% Ne^{20}–0.5% Ne^{22} gas mixture.

experimentally measured wave intensities and difference frequencies with the theoretical plots for an equal mixture of two Ne isotopes of masses 20 and 22. The intensity curves of the two traveling waves are identical. No wave extinction and no power dip is observed in single mode and in multimode operation, in agreement with the theory. The difference frequency varies smoothly across the nearly 500 Mc/sec region observed, as predicted by the theory. However, the magnitudes of the observed difference frequency errors are larger than the computer values.

V. CONCLUSIONS

The experimental measurements of traveling-wave amplitudes and difference frequencies are in good qualitative agreement with the theory of Aronowitz and Heer. The presence of a slight but unavoidable difference between the two traveling waves in their gain-to-loss ratios gives rise to interesting wave extinction and mode-pulling effects. The dependence of these effects on cavity frequency and laser power are in general agreement with the theory.

Unidirectional oscillations occur for each symmetric placement of cavity modes due to the strong competition for atoms between the two oppositely directed traveling

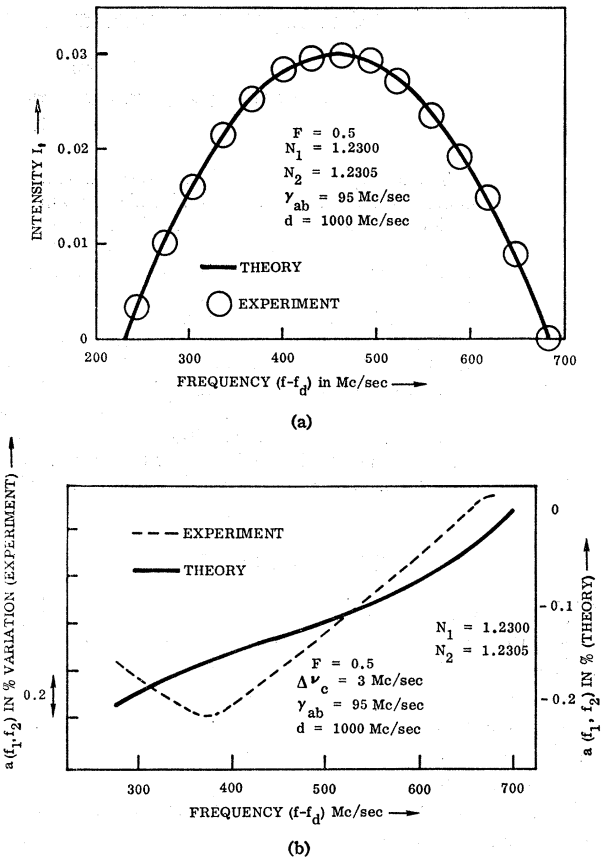

FIG. 11. Comparison of theoretical to experimental traces of (a) traveling-wave intensity and (b) difference frequency for a 50% Ne^{20}–50% Ne^{22} gas mixture.

waves. The wave with the higher cavity loss is extinguished at each $\frac{1}{2}\lambda$ cavity length interval.

Detection of the amplitude modulation of the intensity of one of the traveling waves is a convenient method for measuring the difference frequency. The phase difference between the amplitude signal and the heterodyne beat signal was observed to vary by less than 180 deg over one mode spacing. The frequency error associated with this phase difference is much smaller than any error due to variation in mode pulling effects.

The use of a laser tube containing an equal mixture of Ne^{20} and Ne^{22} isotopes reduces considerably the effects of mode competition and mode pushing and pulling on the traveling-wave amplitudes and frequencies.

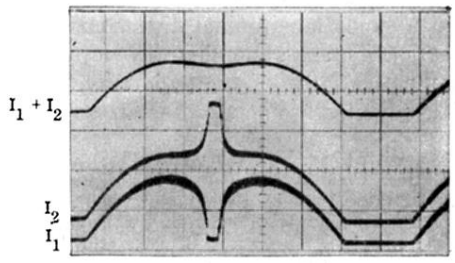

FIG. 2. Experimental display of oppositely directed traveling wave intensities I_1, I_2 and sum intensity I_1+I_2 versus cavity tuning showing amplitude modulation and extinction phenomena in single mode operation. The mode spacing is 510 Mc/sec.

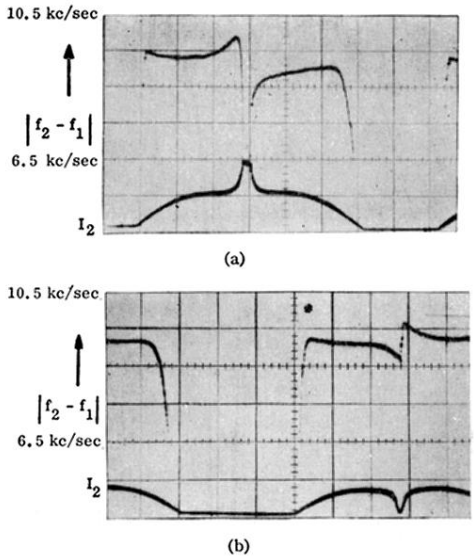

FIG. 4. Experimental displays of difference frequency and wave intensity for (a) the counterclockwise wave dominant and (b) the counterclockwise wave extinguished at the center of the gain curve.

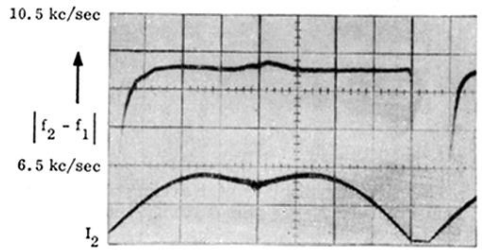

FIG. 6. Experimental display of difference frequency (top) and one wave intensity (bottom) for nearly identical traveling-wave intensities.

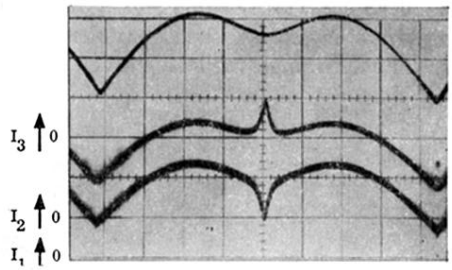

FIG. 8. Experimental displays of traveling-wave intensities I_1, I_2, and sum intensity I_1+I_2 versus cavity tuning showing two-mode extinction effects.

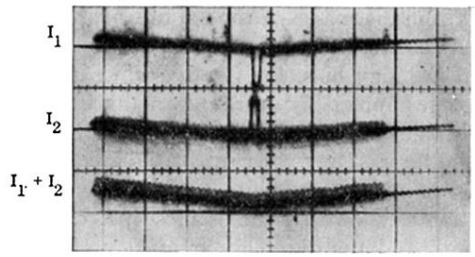

FIG. 9. Enlargement, showing shape and width of two-mode extinguishing region. The frequency scale is 7 Mc/sec per division.